BREAST

Correlation of contrast-enhanced ultrasound kinetics with prognostic factors in invasive breast cancer

**Botond K. Szabó · Ariel Saracco · Ervin Tánczos ·
Peter Aspelin · Karin Leifland · Brigitte Wilczek ·
Rimma Axelsson**

Abstract

Objectives To correlate contrast-enhanced ultrasound (CEUS) kinetic parameters with traditional and molecular prognostic factors in invasive breast cancer.
Methods Seventy-five invasive breast cancers were evaluated with contrast harmonic imaging after the injection of a bolus dose of 2.4 ml sulphur hexafluoride microbubble contrast agent. The lognormal function was used for quantitative analysis of kinetic data. These parameters correlated with traditional prognostic factors (tumour size, histological type, tumour grade, axillary lymph node status) and immunohistochemical biomarkers (ER, PR and HER2 status).
Results Statistically significant correlation was found between time-to-peak and tumour grade (*P* value=0.023), PR status (*P* value=0.042) and axillary node status (*P* value=0.025). Washout ratio, measured at 21 s was significantly associated with ER status (*P* value=0.042) and PR status (*P* value=0.026).

Conclusions Invasive breast carcinomas exhibiting earlier peak enhancement and faster elimination of microbubble contrast agent at CEUS are found to be associated with established predictors of poor prognosis.
Key Points
• *Contrast-enhanced ultrasound (CEUS) can potentially determine the aggressiveness of invasive breast cancers.*
• *Early peak enhancement and accelerated wash-out at CEUS suggest poor prognosis.*
• *CEUS kinetics are similar to that of DCE-MRI in assessing tumour aggressiveness.*

Introduction

High-resolution conventional grey-scale ultrasound is an essential part of breast and axillary imaging, especially in young patients and mammographically dense glandular breasts [1]. Microbubble contrast agents have been shown to be useful in demonstrating abnormal vasculature at colour and power Doppler ultrasound and allow differentiation of benign lesions from malignant breast masses [2]. Recent advances in ultrasound machines and dedicated software applications along with modern contrast agents like SonoVue have led to the ability to detect microvasculature at the capillary level. Compared with Doppler ultrasound, contrast-enhanced ultrasound (CEUS) offers better sensitivity in the visualisation of pathological microvessels in neoplastic tissues [3].

Previous studies showed that both dynamic contrast-enhanced (DCE) computed tomography (CT) and magnetic resonance imaging (MRI) methods are able to assess tumour microcirculation non-invasively [4]. As angiogenesis correlates well with biological behaviour of tumours and disease outcome, DCE-CT and MRI features can also provide

B. K. Szabó (✉)
Department of Radiology, Faculty of Medicine, University of Szeged, 6725 Szeged, Semmelweis u. 6., Hungary
e-mail: raeszabb@gmail.com

A. Saracco · P. Aspelin · R. Axelsson
Division of Medical Imaging and Technology, Department of Clinical Science, Intervention and Technology (CLINTEC), Karolinska Institutet, Stockholm, Sweden

E. Tánczos
Bolyai Institute, Faculty of Science and Informatics, University of Szeged, Szeged, Hungary

E. Tánczos
Department of Medical Physics and Informatics, Faculty of Medicine, University of Szeged, Szeged, Hungary

K. Leifland · B. Wilczek
Division of Radiology, Department of Breast Imaging, Unilabs Capio S:T Göran Hospital, Stockholm, Sweden

information on tumour aggressiveness and prognosis [5, 6]. A further application area of DCE imaging methods that evaluate vascular properties of tumours is the monitoring of treatment in cancer [7].

Unlike MR contrast agents that distribute into both intra-vascular and extracellular spaces, microbubble ultrasound contrast agents are solely intravascular in nature, therefore reflecting blood flow only. Looking at the potential applications of dynamic MR/CT and CEUS, there are, however, more similarities than differences. In breast imaging, CEUS has a potential in characterising mass lesions, staging invasive cancer, detecting tumour recurrence and assessing response to neoadjuvant chemotherapy [8, 9]. Correlation between dynamic MR features and prognostic factors has been investigated in breast cancer [10, 11]. CEUS parameters have only been studied as possible prognostic markers in tumours other than breast cancer [12, 13], or in metastatic lymph nodes from breast cancer [14]. To our knowledge, there are no published studies examining the prognostic value of CEUS kinetics in breast tumours in vivo.

The aim of the study was to correlate CEUS kinetic parameters with traditional and molecular prognostic factors in invasive breast cancer.

Materials and methods

Patient material

Approval from the Regional Ethics committee was obtained for this study. All patients were informed about the study and gave their oral consent.

A total of 74 patients (74 women; mean age 58 years; range, 37–81 years) with 75 breast tumours were evaluated between March 2007 and September 2009.

The inclusion criteria were: age of 18 years or more with a definite malignant appearance (ACR BI-RADS 5) detected primarily with mammography, ultrasound or both. Exclusion criteria were pregnancy or lactation, known allergy to the contrast agent (sulphur hexafluoride) and severe cardio-pulmonary disease.

Of the 75 lesions included in our study, 35 were palpable and 40 were non-palpable. Asymptomatic patients were recruited from screening mammography, and palpable lesions from the symptomatic breast clinic. All patients underwent ultrasound examination of the axillae. Pathological axillary lymph nodes found on ultrasound were confirmed with imaging-guided fine-needle aspiration biopsy (FNAB). All patients with clinically positive nodal status underwent axillary lymph node dissection, whereas sentinel node biopsy was performed in patients with clinically negative axilla.

Imaging methods

Mammography was performed using analogue equipment (Mammomat 3000 Nova; Siemens Erlangen, Germany/Planmed Sophie; Planmed, Helsinki, Finland/Senographe 800 T; GE, Milwaukee WI, USA) and full-digital equipment (MicroDose mammography; Sectra Stockholm, Sweden) using the three standard views: craniocaudal (CC), mediolateral oblique (MLO) and latero-medial (LM), and some additional views were acquired when needed (spot compression, magnification or supplementary views). The fundamental ultrasound examination in B mode was performed using a Philips iU22 (Philips Medical Systems, Eindhoven, The Netherlands) using a high-resolution multifrequency linear probe L17-5 MHz and special techniques SonoCT (real-time compound imaging, crossbeam imaging) and XRES (speckle, noise and clutter reduction imaging). Image acquisition with power Doppler was performed in all tumours as a standard procedure, with the intention of getting adequate and optimal detection of vascularity that was then used as the imaging plane for real-time contrast harmonic imaging (CHI) ultrasound. With the help of Doppler imaging, the most vascularised portion of the tumour was chosen for CEUS imaging.

Contrast-enhanced ultrasound was performed using real-time grey-scale CHI (CHI+FI, images side by side) ultrasound with the same equipment (Philips iU22, software Vision 2007–2009) using a multifrequency L9-3 MHz linear probe, especially designed for this purpose.

Second-generation microbubble (MB) contrast agent (sulphur hexafluoride, Sono Vue; Bracco, Milano, Italy) was injected through a 21-G catheter via the antecubital vein.

An injection of 2.4 ml MB was administered manually as a bolus (2 s), followed by a flush of 10 ml saline solution. The examination was recorded from the start of the bolus and for a 120-s period.

The lesion biopsies were performed after the ultrasound examination at the same visit; therefore CEUS results were not affected by the biopsy.

During CHI, a low MI of 0.06 was used in all cases, as well as applying minimal compression to the breast, to avoid bursting microbubbles.

Evaluation of images

CEUS studies were saved in the ultrasound hard disc system, and then transferred to a PC for further quantitative analyses with advanced ultrasound quantification software (Q LAB 7.0; Philips Medical Systems, Seattle WA, USA). The computer-assisted program, with the help of a "whole tumour ROI" delineating every tumour, allowed acquisition of time (s) / signal intensity (db) curves. In our study, raw kinetic curves acquired in the first 50 s after the appearance of contrast medium, were used for data analysis.

Prospective mage analysis was performed by two experienced radiologists (A.S., B.S.).

Analysis of time–signal intensity curves

The lognormal function was used to fit the raw CEUS time–signal intensity curves, in all 75 tumours. Mathematical modelling of contrast kinetics made it possible to quantitatively assess tumour microvascular blood flow with the calculation of different parameters [15]:

$$I(t) = \frac{AUC}{\sqrt{2\pi}\sigma(t-t_0)} e^{\frac{[\log(t-t_0)-\mu]^2}{2\sigma^2}} + I_0, \quad \text{with } t > t_0$$

$$\text{MTT} = e^{\mu+\frac{\sigma2}{2}}, \quad t_p = e^{\mu-\sigma2}$$

where $I(t)$ is the backscattered signal intensity as a function of time. The parameters μ and σ are the indicators of location and shape of the lognormal distribution. Horizontal scaling of the curve can be done by changing μ: with fixed σ, the greater the μ, the slower the wash-in and wash-out rate will be. Whereas the skewness of the curve is determined by σ, with fixed μ; the greater the σ, the faster the wash-in and slower the wash-out rate will be. I_0 is the baseline intensity, and t_0 is the arrival time of the contrast medium bolus. This model allows the determination of haemodynamics-related parameters as the area under the curve (AUC), mean transit time (MTT) and time to peak signal intensity (t_p). Mean transit time is the average time the contrast agent at a given dose spends in the tumour vessels, whereas time to peak signal intensity (time-to-peak) is the time elapsed between the first appearance of contrast agent and maximum signal intensity value of the kinetic curve. Curve maximum (C_{max}) was defined as the intensity maximum on a fitted curve after subtraction of intensity offset. Another curve maximum was used, where C_{max} was standardised to AUC (standardised curve maximum [C_{max-sd}]). Conventional parameters wash-out ratios at 21 and 50 s were calculated using the fitted lognormal curves (model-based wash-out ratios, W_{21m} and W_{50m}). Wash-out ratio is an established quantitative parameter that is used to describe the downslope of kinetic curves. It gives the relative signal intensity decrease from the peak to the endpoint of the curve.

$$W_{21m} = \frac{SI_{peak}-SI_{21}}{SI_{peak}} \times 100 \quad W_{50m} = \frac{SI_{peak}-SI_{50}}{SI_{peak}} \times 100$$

where W_{21m} and W_{50m} are the model-based wash-out ratios, SI_{peak} is peak signal intensity, SI_{21} and SI_{50} are signal intensities on the fitted time–signal intensity curves at 21 and 50 s, respectively. Wash-out ratios measured at 21 and 50 s appeared to be important in discriminating benign from

malignant breast lesions in a previous paper [16], therefore we calculated both parameters in our recent study as well.

Histopathological and immunohistochemical analysis

All patients included in this study underwent surgical excision and histopathological verification of the excised specimen was performed. Tumour size was measured microscopically; it was defined as the maximum diameter of the largest invasive focus. Histological typing of tumours was performed according to the WHO classification. Tumour grade was determined using the Elston–Ellis grading system. Axillary lymph node status was considered to be positive when the histopathological examination of the excised lymph node showed metastatic involvement.

Oestrogen (ER) and progesterone receptor (PR) status of the tumours was also determined as part of the routine practice, classifying tumours into 0 = negative, 1+ = low, 2+ = intermediate and 3+ = highly positive groups. In our institution the cut-off value of 1 % was used, 0 = defined as ER/PR negative—less than 1 % positive invasive tumour nuclei in the sample tested with immunohistochemistry (IHC). The categories 1+, 2+ and 3+ were all considered to be positive (more than or equal to 1 % positive invasive tumour nuclei in the sample tested with IHC).

HER2 immunohistochemical staining was classified as 0 = negative, 1+ = low, 2+ = intermediate or 3+ = highly positive. Tumours with 2+ or 3+ staining were considered HER2-positive, and tumours with 0 or 1+ were negative in this study. Fluorescent in situ hybridisation (FISH) was performed for samples with HER2 2+ and 3+ staining (in 19 cases), which confirmed the amplification of the HER2-gene in 6 (31.5 %) cases. HER2 receptor analysis was performed according to the American Society of Clinical Oncology/College of American Pathologists (ASCO-CAP) guidelines [17].

The following antibodies were used for immunohistochemical analysis: Ventana RTU klonSP1 for ER, Ventana RTU klon1E2 for PR and Ventana PATHWAY4B5 for HER2.

Statistical analysis

Spearman's rank correlation test was performed to identify relationships between continuous and ordinal variables. Pearson's correlation was used for the comparison of two interval variables. One-way analysis of variance was applied to correlate nominal data with continuous variables. Dichotomous prognostic factors were correlated with kinetic parameters using the Wilcoxon rank-sum test (which is equivalent to Mann-Whitney U test).

Where more than one significant correlation was found at univariate analysis, multivariate tests were performed to choose the most significant predictors of a dependent

variable. In our study, for binary dependent variables (PR status and axillary node status), logistic regression was performed using a backward covariate selection method.

Statistical significance was established at a P value of <0.05, whereas a "trend" towards statistical significance was defined as P value of >0.05 and <0.1. Bonferroni correction of the P values obtained was not applied owing to the exploratory nature of the study and, also, to a relatively small sample size.

The software package Mathematica, version 8 (Wolfram Research, Champaign, IL, USA) was used for curve fitting. Data extraction, calculation of parameters and statistical analysis was performed using the R statistical language and environment for Linux (version 2.10.1).

Results

Prognostic factors

Histopathological analysis of the 74 patients with 75 malignant lesions showed invasive ductal carcinoma not otherwise specified in 57 patients (76 %), invasive lobular carcinoma in 12 (16 %), invasive tubular carcinoma in 4 (5.3 %), invasive mucinous carcinoma in 1 (1.3 %) and invasive papillary carcinoma in 1 (1.3 %). According to the Elston–Ellis grading system, there were 17 (22.6 %) grade I tumours, 42 (56 %) grade II and 16 (21.3 %) grade III. The size of the tumours ranged from 4 to 45 mm and the mean size was 18.36 mm. There were 7 (9.3 %) ER-negative tumours, 21 (28 %) PR-negative and 6 (8 %) HER2-positive.

Of the 74 patients, ultrasound identified pathological lymph nodes in the ipsilateral axilla in 28 cases (the patient with two foci of cancer had negative axilla). Of these 28 cases, lymph nodes were palpable in 25 cases and impalpable in 3 cases. The axilla was found to be negative on physical examination and ultrasound in 46 patients. Among these, sentinel node biopsy revealed four additional cases of axillary lymph node involvement. Altogether there were 32 malignant tumours with associated histologically proven axillary lymph node metastasis.

Correlation between kinetic parameters and prognostic factors

Statistically significant correlation was found between model-based time-to-peak (t_p) and tumour grade (Spearman's rank correlation, P value=0.023); t_p appears to be shorter in more aggressive tumours (Fig. 1). The difference in t_p between PR-negative and PR-positive tumours was statistically significant; t_p was found to be significantly shorter in the PR-negative group (Wilcoxon rank sum statistic, W=394, P value=0.042). The comparison of t_p with axillary node status showed that t_p
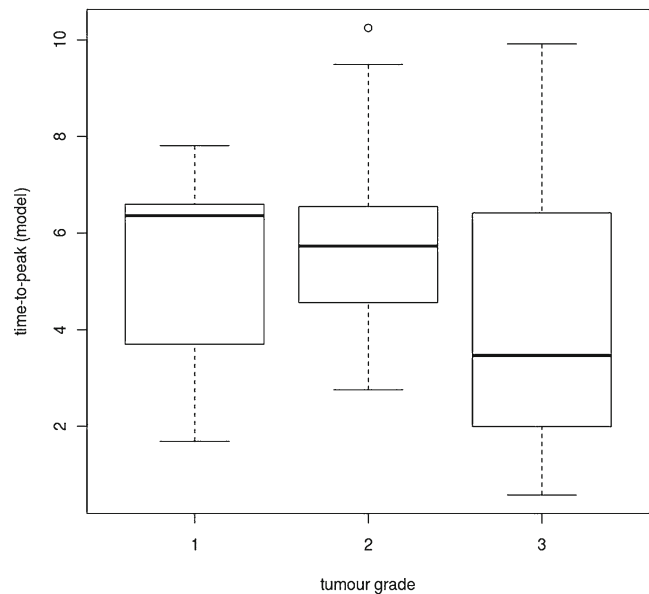

Fig. 1 The relationship between model-based time-to-peak (t_p) and tumour grade (Spearman's rank correlation, rho=-0.26, P value=0.023). Shorter time-to-peak (t_p) represents a more aggressive tumour

is shorter in node-positive tumours, after replacing an outlier (case 39) with the mean this difference was statistically significant (Wilcoxon rank sum statistic, W=897, P value=0.025, Fig. 2). The model-based wash-out ratio, measured at 21 s (W_{21m}) was found to be significantly higher in the ER-negative than the ER positive tumours (Wilcoxon rank sum statistic, W=350, P value=0.042). Similar correlation was found between W_{21m} and PR status, W_{21m} appeared to be significantly greater in PR-negative than PR-positive tumours (Wilcoxon rank sum statistic, W=756, P value=0.026) (Fig. 3).

Kinetic parameters C_{max} (curve maximum, Wilcoxon rank sum statistic, W=923, P value=0.012) and AUC (area under the curve Wilcoxon rank sum statistic, W=904, P value=0.02) also showed significant correlation with axillary node status, although it should be noted that lower C_{max} and AUC values were associated with positive axillary status.

Typical enhancement curves of low- and high-grade invasive breast cancers are shown in Fig. 4.

Notable trends towards statistical significance were observed in the following correlations: between the lognormal parameter μ and PR status of tumours (μ appears to be decreased in PR-negative tumours; Wilcoxon rank sum statistic, W=417, P value=0.079), between wash-out ratio W_{50m} and ER status (W_{50m} appears to be greater in ER-negative tumours; Wilcoxon rank sum statistic, W=330, P value=0.095), between MTT and ER status (MTT appears to be decreased in ER-negative tumours; Wilcoxon rank sum statistic, W=140, P value=0.075).

The correlation between contrast-enhanced ultrasound kinetic parameters derived from a lognormal model and prognostic factors is shown in Table 1. For further comparison,
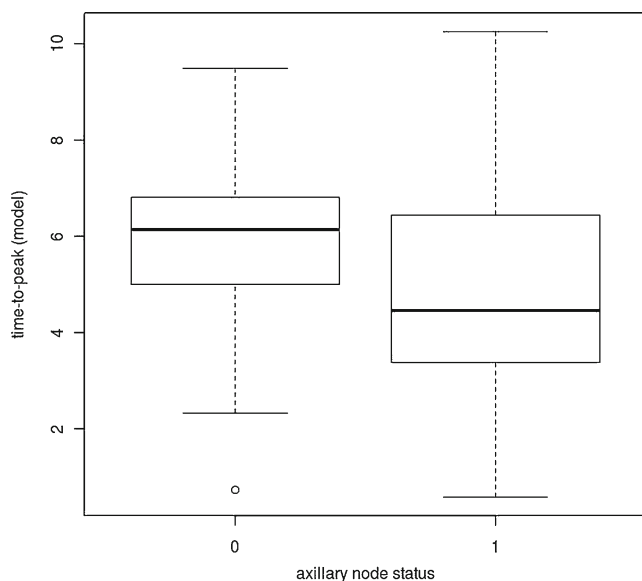
Fig. 2 The relationship between model-based time-to-peak (t_p) and axillary lymph node status. Time-to-peak (t_p) is significantly shorter in node-positive tumours (after replacing an outlier with the mean, Wilcoxon rank sum statistic $W=897$, P value$=0.025$)

mean values of kinetic parameters in different prognostic groups are shown in Table 2.

Multivariate analysis

Kinetic parameters found to be significant at the exploratory univariate tests were used in the multivariate models. Two models were constructed for binary logistic regression: the first model was included time-to-peak (t_p) and wash-out ratio W_{21m}, in which the dependent variable was PR status; whereas in the second model, t_p, area under the curve (AUC) and curve maximum (C_{max}) were tested against axillary node status. No multivariate models were made for tumour grade and ER status, because there was only one statistically significant correlation in each dataset.

In the first model, W_{21m} was retained in the equation and proved to be an independent predictor of PR status (Wald z-statistic$=-2.11$, P value$=0.034$), but t_p was rejected from the model. In the second regression model, where axillary node status was the dependent variable, C_{max} retained its significance (Wald z-statistic$=-2.15$, P value$=0.031$). Kinetic parameters t_p and AUC were rejected from the model.

Discussion

Angiogenesis is a normal physiological process in embryonic vascular development, but also plays an important role in wound healing and reproduction in health. Abnormal regulation of angiogenesis can occur in a number of pathological conditions including malignancies, inflammatory and
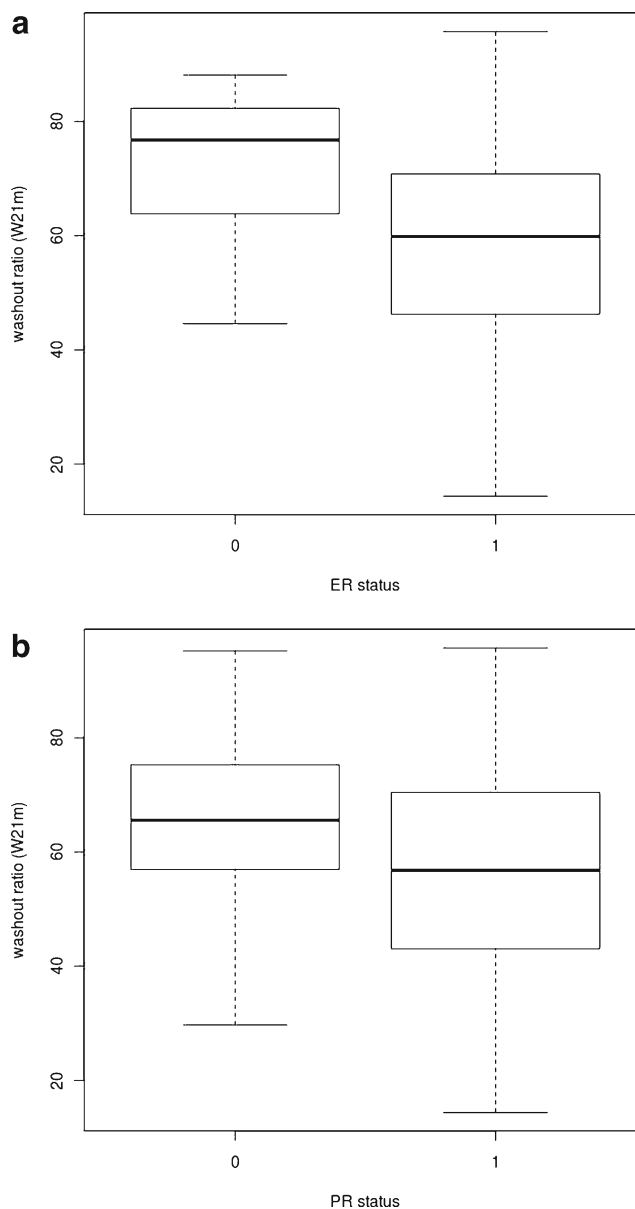

Fig. 3 The relationship between W_{21m} (model-based wash-out ratio at 21 s) and (**a**) ER or (**b**) PR status. W_{21m} is significantly greater in ER-negative and also in PR-negative tumours (for ER status, Wilcoxon rank sum statistic $W=350$, P value$=0.042$, for PR status $W=756$, P value$=0.026$)

autoimmune diseases, asthma, diabetes, cirrhosis, multiple sclerosis, endometriosis, stroke and ischaemic heart disease, but the list is far from being complete [18]. First Folkman hypothesised in 1971 that the growth and spread of malignant tumours are highly dependent upon the formation of new vessels [19]; angiogenesis has been one of the most extensively researched topics in biomedical science ever since. Tumour expansion facilitates the release of several angiogenic growth factors, of which vascular endothelial growth factor (VEGF) is the one most often studied. The main steps that comprise the process of angiogenesis are the growth,

Fig. 4 The lognormal function was used for mathematical modelling of time–signal intensity curves in contrast-enhanced ultrasound of breast cancer. **a** A grade I, ER-positive, axillary status negative—typically low-grade invasive cancer (case no. 46) showing relatively slower wash-in and lengthened wash-out. **b** A grade III, ER-negative, axillary node-positive—typically high-grade invasive cancer (case no. 66) showing faster wash-in and accelerated wash-out
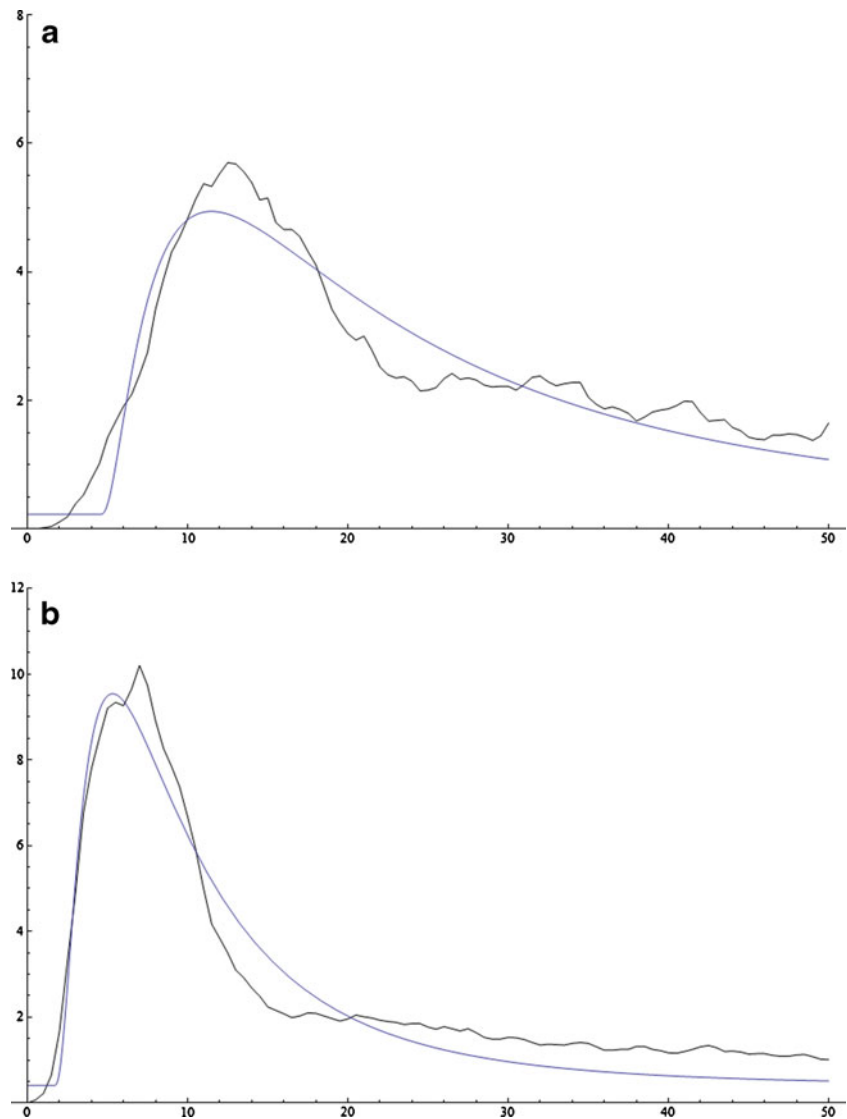
migration and differentiation of endothelial cells. These newly formed pathological microvessels in tumours are largely different from normal capillaries. This vascular network shows perivascular detachment, irregular shape, abnormal calibre and the lining is composed of fenestrated endothelial cells. These changes usually lead to altered perfusion, increased permeability and lacking regulatory processes of normal vessels.

Modern radiology provides a number of imaging methods that are capable of the non-invasive assessment of tumour-associated angiogenesis. In breast imaging, DCE-MRI has emerged as a powerful supplementary tool for the detection of cancer [20]. Gadolinium-based contrast agents are intravascular and extracellular in distribution, therefore enhancement kinetics are influenced by both tumour perfusion and permeability of microvessels. Although there is a considerable overlap in contrast dynamics of benign and malignant breast tumours, kinetic DCE-MRI features help the differentiation of benign from cancerous tissue [21]. MR contrast

perfusion is usually faster and, owing to increased vascular permeability, enhancement is stronger in malignant breast tissues compared with benign abnormalities. Altered perfusion in malignant tumours results in faster initial contrast enhancement (wash-in), peak-enhancement is observed earlier, and accelerated elimination of contrast (wash-out) is demonstrated; whereas benign lesions tend to show slower contrast medium uptake, the peak occurs later, and enhancement curves often exhibit a steady increase [22]. Unlike MR contrast media, microbubble contrast agents used in CEUS remain in the vasculature leading to somewhat different time–signal intensity curves, but the basic perfusion patterns are compatible with that of DCE-MRI. This allows CEUS to evaluate angiogenesis quantitatively [23]; furthermore, CEUS kinetics can discriminate benign from malignant breast lesions similar to MRI [8, 24].

It is difficult to quantify tumour neovascularisation, but microvessel density (MVD) and VEGF expression have

Table 1 Correlation of contrast-enhanced ultrasound kinetic parameters derived from a lognormal model with prognostic factors

	Histological type[a]	Tumour size[b]	Tumour grade[c]	ER status[d]	PR status[d]	HER2 status[d]	Axillary node status[d]
C_{max}	0.108	0.199	0.404	0.792	0.186	0.145	0.012
$C_{max\text{-}sd}$	0.716	0.577	0.786	0.090	0.087	0.271	0.662
AUC	0.125	0.354	0.308	0.591	0.086	0.130	0.020
μ	0.163	0.491	0.954	0.172	0.079	0.145	0.936
σ	0.176	0.660	0.207	0.193	0.684	0.667	0.692
t_p	0.796	0.244	0.023	0.906	0.042	0.519	0.025[e]
W_{21m}	0.797	0.614	0.547	0.042	0.026	0.287	0.1765
W_{50m}	0.297	0.316	0.692	0.095	0.342	0.353	0.811
MTT	0.368	0.841	0.575	0.075	0.392	0.296	0.810

Numbers are *P* values

Parameters determined by the lognormal model: C_{max} curve maximum=peak signal intensity, $C_{max\text{-}st}$ curve maximum standardised to AUC, *AUC* area under the time-signal intensity curve, μ lognormal model parameter for horizontal scaling of the curve (increasing μ will result in slower wash-in and wash-out), σ lognormal model parameter determining the skewness of the curve, t_p model-based time-to-peak, W_{21m} model based-wash-out ratio at 21 s, W_{50m} model-based wash-out ratio at 50 s, *MTT* mean transit time

[a] Analysis of variance, interval vs nominal data

[b] Pearson's correlation, interval vs interval data

[c] Spearman's rank correlation, interval vs ordinal data

[d] Wilcoxon rank sum test, equivalent to Mann-Whitney *U* test / interval vs dichotomous data

[e] Correlation after replacing an outlier (case 39, 103.86) with mean (6.69)

been repeatedly proposed as prognostic markers for breast cancer [25, 26]. MR contrast enhancement in breast tumours was found to be related to VEGF expression [27], and several studies have demonstrated correlation between MVD and MR features as well [28, 29]. Previous research has shown that MR contrast kinetics correlate significantly with established prognostic factors and biomarkers in breast cancer [10, 11]. Furthermore, elevated DCE-MRI parameters related to increased tumour perfusion and vascular permeability were shown to be predictive of shorter disease-free and overall survival of breast cancer patients [30, 31].

Similar to DCE-MRI, CEUS imaging also has the ability to yield insight into tumour-associated angiogenesis, but contrast-enhanced ultrasound parameters are not affected by changes in vascular permeability and appear to be related more closely to MVD than VEGF expression [32]. In malignancies other than breast cancer, CEUS has already been studied as a potential prognostic tool. It has been pointed out that certain CEUS enhancement patterns show significant correlation with Ki-67 proliferative index in hepatic metastases from neuroendocrine tumours [13] and, also, tumour vascularisation at CEUS appeared to be a predictor of survival of patients with pancreatic adenocarcinoma [12]. To our knowledge, there has only been one study that investigated the role of CEUS in predicting the aggressiveness of breast cancer, but researchers examined contrast enhancement in lymph nodes and CEUS enhancement patterns were correlated with HER2 and lymph node stage [14].

In our study, quantitative CEUS kinetic parameters measured in invasive breast cancers were compared using different traditional and immunohistochemical prognostic variables that are used routinely in clinical practice. We observed that tumours with shorter time-to-peak were more likely to have higher histological grade, negative PR status and metastatic involvement of the axillary lymph nodes. Wash-out ratio measured at 21 s after the appearance of contrast medium was also significantly associated with ER and PR status. There were further notable trends towards statistical significance in other comparisons: decreased lognormal parameter μ, increased wash-out ratio measured at 50 s and shorter MTT are likely to be associated with established predictors of poorer prognosis. According to our findings, increased tumour perfusion—that is shown by faster wash-in and accelerated wash-out—appears to be an indicator of worse prognosis in invasive breast cancer.

At univariate analysis there were two significant correlations that are difficult to explain: model-based curve maximum (C_{max}, peak intensity) and area under the curve (AUC) also showed association with axillary node status, although boxplots showed that both C_{max} and AUC were lower in tumours with positive than negative nodal status. We assume that these correlations are incidental and presumably due to the relatively small sample size. Multivariate statistics showed that wash-out ratio at 21 s is a stronger predictor of PR status than time-to-peak (t_p). Time-to-peak was rejected from the second multivariate model as well, where the

Table 2 Comparison of contrast-enhanced ultrasound kinetic parameters derived from a lognormal model with prognostic factors (numbers are mean values with standard deviation *in parentheses*)

	Tumour grade			ER status		PR status		HER2 status		Axillary node status	
	I	II	III	neg.	pos.	neg.	pos.	neg.	pos.	neg.	pos.
C_{max}	13.42 (15.26)	19.05 (19.06)	10.48 (13.78)	14.59 (15.73)	16.08 (17.69)	11.79 (14.21)	17.55 (18.39)	15.41 (17.41)	22.05 (17.94)	19.8 (18.61)	10.75 (14.38)
$C_{max\text{-}sd}$	0.054 (0.031)	0.066 (0.039)	0.059 (0.029)	0.08 (0.037)	0.06 (0.035)	0.073 (0.04)	0.057 (0.032)	0.063 (0.036)	0.046 (0.027)	0.062 (0.037)	0.061 (0.032)
AUC	673 (1364)	466 (603)	392 (950)	375 (617)	510 (919)	281 (486)	581 (999)	450 (821)	1043 (1492)	586 (953)	378 (804)
μ	2.89 (0.93)	2.59 (0.47)	2.8 (0.83)	2.41 (0.59)	2.73 (0.69)	2.47 (0.46)	2.79 (0.74)	2.67 (0.64)	3.11 (1.04)	2.65 (0.57)	2.78 (0.81)
σ	0.98 (0.38)	0.87 (0.32)	1.99 (0.5)	0.8 (0.37)	0.98 (0.4)	0.95 (0.35)	0.97 (0.41)	0.95 (0.38)	1.09 (0.59)	0.92 (0.33)	1.02 (0.47)
t_p	11.22 (23.94)	5.89 (1.76)	4 (2.66)	5.61 (2.47)	6.8 (12.12)	4.68 (2.18)	7.47 (13.52)	6.77 (12.04)	5.85 (2.7)	5.79 [a] (1.84)	4.87 [a] (2.39)
W_{21m}	54.87 (21.4)	58.86 (19.94)	59.94 (18.93)	71.66 (16.14)	56.8 (19.81)	66.19 (15.42)	55.07 (20.67)	58.88 (19.87)	50.23 (20.04)	55.72 (20.68)	61.49 (18.57)
W_{50m}	81.25 (21.63)	87.79 (9.21)	86.87 (7.43)	91.04 (7.91)	85.6 (13.24)	89.57 (6.78)	84.76 (14.44)	86.37 (13.09)	83.08 (11.06)	86.5 (11.25)	85.57 (15.02)
MTT	71.89 (101.2)	29.11 (29.81)	174.1 (461.3)	27.8 (40.89)	74.06 (232.2)	28.81 (34.85)	85.66 (259.3)	46.94 (74.05)	331.89 (750.4)	39.14 (58.74)	110.8 (331)

Parameters determined by the lognormal model: C_{max} curve maximum = peak signal intensity, $C_{max\text{-}st}$ curve maximum standardised to AUC, *AUC* area under the time-signal intensity curve, μ lognormal model parameter for horizontal scaling of the curve (increasing μ will result in slower wash-in and wash-out), σ lognormal model parameter determining the skewness of the curve, t_p model-based time-to-peak, W_{21m} model-based wash-out ratio at 21 s, W_{50m} model-based wash-out ratio at 50 s, *MTT* mean transit time

[a] Values were calculated after replacing an outlier (case 39, 103.86) with the mean (6.69)

dependent variable was axillary status, and C_{max} was shown to be independently related to axillary status. Again we believe that our small sample size and relatively weak correlations at univariate analysis had a great influence on multivariate analysis, therefore definitive conclusions cannot be drawn from the multivariate tests.

Owing to the lack of similar published research in the field of CEUS, we can only compare our findings with those of studies that focused on the prognostic value of MR enhancement kinetics. We can assume that the amplitude of MR signal is mainly affected by vascular permeability, but the early appearance of peak enhancement with faster elimination of contrast medium is strongly related to increased tumour perfusion even in DCE-MRI. In this aspect, our results are in accordance with previously presented data. In a previous MRI study [10], shorter time-to-peak enhancement was associated with higher tumour grade, HER2 and ER status; and also, wash-out type enhancement curves showed an association with increased proliferation activity as assessed by Ki-67. Another study demonstrated that early peak enhancement on MRI correlated with negative ER expression [11].

We can hypothesise that the more aggressive a tumour is, the higher its angiogenic activity will be to support its faster expansion. Increased new vessel formation in high-grade tumours may lead to higher MVD, which in turn affects the signal at DCE-MR and CEUS. Furthermore, faster development of microvessels may also result in a chaotic pathological vascular pattern, which possibly influences the formation of more arterio-venous shunts as well. As a result of these factors, blood perfusion will be increased, allowing a contrast bolus to flow quickly though the tumour microvasculature on both DCE-MR and CEUS imaging.

In summary, our study demonstrated that invasive breast carcinomas exhibiting earlier peak enhancement and faster elimination of microbubble contrast medium at CEUS are found to be associated with established predictors of poor prognosis. These promising results suggest that CEUS has the potential to determine the biological behaviour of invasive breast cancers non-invasively, and may also help to identify future clinical application areas for this new imaging method.

whether CEUS kinetics are able to differentiate between benign and malignant tumours.

References

1. Skaane P, Sager EM, Olsen JB et al (1999) Diagnostic value of ultrasonography in patients with palpable mammographically noncalcified breast tumors. Acta Radiol 40:163–168
2. Kedar RP, Cosgrove D, McCready VR, Bamber JC, Carter ER (1996) Microbubble contrast agent for color Doppler US: effect on breast masses. Work in progress. Radiology 198:679–686
3. Delorme S, Krix M (2006) Contrast-enhanced ultrasound for examining tumor biology. Cancer Imaging 6:148–152
4. Cuenod CA, Fournier L, Balvay D, Guinebretière J (2006) Tumor angiogenesis: pathophysiology and implications for contrast-enhanced MRI and CT assessment. Abdom Imaging 31:188–193
5. Lee T, Purdie TG, Stewart E (2003) CT imaging of angiogenesis. Q J Nucl Med 47:171–187
6. Griebel J, Mayr NA, de Vries A et al (1997) Assessment of tumor microcirculation: a new role of dynamic contrast MR imaging. J Magn Reson Imaging 7:111–119
7. Anderson H, Price P, Blomley M, Leach MO, Workman P, Cancer Research Campaign PK/PD Technologies Advisory Committee (2001) Measuring changes in human tumour vasculature in response to therapy using functional imaging techniques. Br J Cancer 85:1085–1093
8. Balleyguier C, Opolon P, Mathieu MC et al (2009) New potential and applications of contrast-enhanced ultrasound of the breast: own investigations and review of the literature. Eur J Radiol 69:14–23
9. Hwang M, Niermann KJ, Lyshchik A, Fleischer AC (2009) Sonographic assessment of tumor response: from in vivo models to clinical applications. Ultrasound Q 25:175–183
10. Szabó BK, Aspelin P, Kristoffersen Wiberg M, Tot T, Boné B (2003) Invasive breast cancer: correlation of dynamic MR features with prognostic factors. Eur Radiol 13:2425–2435
11. Chang Y, Kwon KH, Choi DL et al (2009) Magnetic resonance imaging of breast cancer and correlation with prognostic factors. Acta Radiol 50:990–998
12. D'Onofrio M, Zamboni GA, Malagò R et al (2009) Resectable pancreatic adenocarcinoma: is the enhancement pattern at contrast-enhanced ultrasonography a pre-operative prognostic factor? Ultrasound Med Biol 35:1929–1937
13. Massironi S, Conte D, Sciola V et al (2010) Contrast-enhanced ultrasonography in evaluating hepatic metastases from neuroendocrine tumours. Dig Liver Dis 42:635–641
14. Ouyang Q, Chen L, Zhao H, Xu R, Lin Q (2010) Detecting metastasis of lymph nodes and predicting aggressiveness in patients with breast carcinomas. J Ultrasound Med 29:343–352
15. Strouthos C, Lampaskis M, Sboros V, McNeilly A, Averkiou M (2010) Indicator dilution models for the quantification of microvascular blood flow with bolus administration of ultrasound contrast agents. IEEE Trans Ultrason Ferroelectr Freq Control 57:1296–1310
16. Saracco A, Szabo B, Aspelin P et al (2012) Differentiation between benign and malignant breast tumors using kinetic features of real-time harmonic contrast-enhanced ultrasound. Acta Radiol 53:382–388
17. Shah SS, Ketterling RP, Goetz MP et al (2010) Impact of American Society of Clinical Oncology/College of American Pathologists guideline recommendations on HER2 interpretation in breast cancer. Hum Pathol 41:103–106
18. Carmeliet P (2005) Angiogenesis in life, disease and medicine. Nature 438:932–936
19. Folkman J (1971) Tumor angiogenesis: therapeutic implications. N Engl J Med 285:1182–1186
20. Mann RM, Kuhl CK, Kinkel K, Boetes C (2008) Breast MRI: guidelines from the European Society of Breast Imaging. Eur Radiol 18:1307–1318
21. Kuhl CK (2000) MRI of breast tumors. Eur Radiol 10:46–58
22. Kuhl CK, Mielcareck P, Klaschik S et al (1999) Dynamic breast MR imaging: are signal intensity time course data useful for differential diagnosis of enhancing lesions? Radiology 211:101–110
23. Caproni N, Marchisio F, Pecchi A et al (2010) Contrast-enhanced ultrasound in the characterisation of breast masses: utility of quantitative analysis in comparison with MRI. Eur Radiol 20:1384–1395
24. Zhao H, Xu R, Ouyang Q, Chen L, Dong B, Huihua Y (2010) Contrast-enhanced ultrasound is helpful in the differentiation of malignant and benign breast lesions. Eur J Radiol 73:288–293
25. Uzzan B, Nicolas P, Cucherat M, Perret G (2004) Microvessel density as a prognostic factor in women with breast cancer: a systematic review of the literature and meta-analysis. Cancer Res 64:2941–2955
26. Delli Carpini J, Carpini JD, Karam AK, Montgomery L (2010) Vascular endothelial growth factor and its relationship to the prognosis and treatment of breast, ovarian, and cervical cancer. Angiogenesis 13:43–58
27. Knopp MV, Weiss E, Sinn HP et al (1999) Pathophysiologic basis of contrast enhancement in breast tumors. J Magn Reson Imaging 10:260–266
28. Frouge C, Guinebretière JM, Contesso G, Di Paola R, Bléry M (1994) Correlation between contrast enhancement in dynamic magnetic resonance imaging of the breast and tumor angiogenesis. Invest Radiol 29:1043–1049
29. Buadu LD, Murakami J, Murayama S et al (1996) Breast lesions: correlation of contrast medium enhancement patterns on MR images with histopathologic findings and tumor angiogenesis. Radiology 200:639–649
30. Boné B, Szabó BK, Perbeck LG, Veress B, Aspelin P (2003) Can contrast-enhanced MR imaging predict survival in breast cancer? Acta Radiol 44:373–378
31. Pickles MD, Manton DJ, Lowry M, Turnbull LW (2009) Prognostic value of pre-treatment DCE-MRI parameters in predicting disease free and overall survival for breast cancer patients undergoing neoadjuvant chemotherapy. Eur J Radiol 71:498–505
32. Du J, Li F, Fang H, Xia J, Zhu C (2008) Correlation of real-time gray scale contrast-enhanced ultrasonography with microvessel density and vascular endothelial growth factor expression for assessment of angiogenesis in breast lesions. J Ultrasound Med 27:821–831